

# Comparison of Different Interpolation Methods for Investigating Spatial Variability of Rainfall Erosivity Index

Nazila Khorsandi<sup>1\*</sup>, Mohammad Hossein Mahdian<sup>2</sup>, Ebrahim Pazira<sup>3</sup>, Davood Nikkami<sup>4</sup>, Hadi Chamheidar<sup>5</sup>

<sup>1</sup>Young Researchers club, Takestan Branch, Islamic Azad University, Takestan, Iran

<sup>2</sup>Organization of Research, Education and Extension, Agriculture Ministry, Tehran, Iran

<sup>3</sup>Faculty of Agriculture and Natural Resources, Science and Research Branch, Islamic Azad University, P.O. Box 14515/775, Tehran, Iran

<sup>4</sup>Soil Conservation and Watershed Management Research Institute, Tehran, Iran

<sup>5</sup>Department of soil science, Faculty of Agriculture, Islamic Azad University, Shoushtar Branch, Shoushtar, Iran

Received: 6 November 2011

Accepted: 23 February 2012

## Abstract

The objective of our study was to expand the R factor of the RUSLE model, erosivity index by its estimation from more readily available rainfall erosivity indexes and parameters in stations without rainfall intensity data, and to determine the most accurate interpolation method for preparing an erosivity index map. Among different erosivity indexes and parameters based on rainfall amounts, only the modified fourier Index ( $FI_{mod}$ ) was highly correlated with  $EI_{30}$  in 20 synoptic stations. A local model was used for estimating  $EI_{30}$  from  $FI_{mod}$  in the other 66 stations without rainfall intensity data. The spatial variability of the calculated  $EI_{30}$  in all of the stations was different at an azimuth of  $32^\circ$  when compared to the other directions. Moreover, the nugget-to-sill ratio of the semivariogram (0.27) confirmed a strong spatial correlation of  $EI_{30}$ . The inverse distance weighting (IDW), spline, kriging, and cokriging methods with elevation as a covariable were compared by a cross-validation technique. The root mean square error (RMSE) value of the cokriging method when compared to that of the IDW, kriging, and spline methods in the study area declined by 11%, 3%, and 4%, respectively. The output maps for all of the interpolation methods followed similar decreasing trends from west to east, with the highest erosivity index ( $1,450 \text{ MJ}\cdot\text{mm}\cdot\text{ha}^{-1}\cdot\text{h}^{-1}\cdot\text{y}^{-1}$ ) found in the west. This pattern corresponds with the pattern of climatic change from subhumid to semiarid.

**Keywords:**  $EI_{30}$ , erosivity index, interpolation methods, available parameters of rainfall erosivity

## Introduction

Rainfall erosivity provides the estimation of the forces produced by rainfall to cause water erosion [1]. The rainfall erosivity force (R factor) is one of the basic factors of the universal soil loss equation (USLE) and the revised form of

the USLE. The R factor in these erosion models is the average of summation of storm  $EI_{30}$  during the year. The  $EI_{30}$  factor is the product of total storm energy ( $E$ ) and the maximum intensity measured during 30-minute periods  $I_{30}$ .

Estimation of the  $EI_{30}$  index requires intensity data series over a long period of time at short time intervals, but access to such data is limited in many parts of the world, especially in Iran. Rainfall amount data such as annual,

---

\*e-mail: khorsandi@tiau.ac.ir

monthly, and daily rainfall are more readily available in many stations. A combination of these parameters as readily available indexes can be used. A number of studies have presented relationships between indexes on the basis of rainfall intensity and amount. These relationships can be used for generalizing rainfall erosivity indexes on the basis of intensity in more places. In a tropical watershed in the Colombia lands, Hoyos et al. [2] estimated the annual  $EI_{30}$  from rainfall amounts for ten stations without rainfall intensity data by using two equations for wet and dry seasons. Moreover, in other research a comparison of modeling between the monthly  $EI_{30}$  and Fournier index, storm rainfall, storm duration, and monthly rainfall values for days with  $\geq 10$  mm ( $rain_{10}$ ) and the number of days in a month with rainfall  $\geq 10$  mm ( $day_{10}$ ) was carried out. Models using  $rain_{10}$  and  $day_{10}$  for the estimation of the monthly  $EI_{30}$  have been presented for the least root mean square error (RMSE) and percentage error (PE) [3].

Interpolation methods are tools for estimating unknown values from data observed at known locations. Due to sparse synoptic stations, it is necessary to estimate the erosivity index for regions between stations to prepare maps. Interpolation techniques can be divided into deterministic and stochastic models. In this relation, inverse distance weighting (IDW) and radial basis functions (RBF) are based on deterministic models, and kriging and cokriging are based on stochastic models. Kriging and cokriging methods using the autocovariance structure present in semivariograms. Semivariograms display the similarity degree of regionalized variables over a determined distance, lag  $\alpha$  [4].

Some studies have compared different interpolation methods. Goovaerts [5] compared three geostatistical algorithms (including simple kriging) with varying local means, kriging with external drift, and collocated ordinary cokriging. Among these geostatistical algorithms, the best results are obtained with ordinary cokriging. Cross-validation results have shown that the accuracy of different geostatistical techniques can vary greatly. Another study has demon-

strated that the local polynomial algorithm is better than the IDW method for the investigation of rainfall erosivity in a tropical watershed [2]. Zhang et al. [6] found that the Disjunction Kriging method has more accuracy than Ordinary Kriging and Simple Kriging methods for analysis spatial pattern of rainfall erosivity in Fujian Province. Other research by Men et al. [7] has shown that secondary order of ordinary kriging produced the best results, and the first order of ordinary kriging in Hebei Province.

In relation to the estimation of monthly rainfall, Lloyd [8] applied elevation as a secondary variable by kriging with external drift. Hourly precipitation was interpolated by Verworn and Haberlandt [9] with the additional variable including topography rainfall data from the denser networks and weather radar. This research presented that different types of semivariogram had low impact on performance of interpolation. Also, Diodato and Ceccarelli [10] have compared IDW, ordinary kriging and ordinary cokriging for spatial variability of precipitation. They concluded that cokriging by elevation as co-variable is the best method for interpolation, especially in mountainous regions because precipitation is a geomorphologic feature.

As seen, there are several studies that investigate interpolation methods for estimating the rainfall amounts and rainfall erosivity index. There is not much research that compares different types of interpolation methods, including deterministic and stochastic approaches for estimation rainfall erosivity index and produces a reliable map of the erosivity index. The objectives of this study were as follows:

- 1) to estimate  $EI_{30}$  from more readily available parameters and indexes
- 2) to analyze and model the spatial variability of the  $EI_{30}$  index
- 3) to prepare a map of sparsely measured  $EI_{30}$  values and to characterize the reliability of this map
- 4) to select the best interpolation technique

The results of this study created an optimal erosivity index map that can be used in decision-making processes for the evaluation of soil erosion.

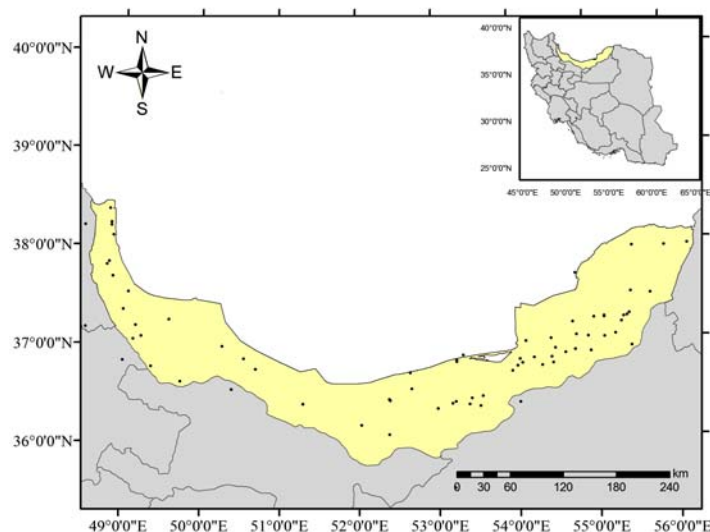


Fig. 1. The location of the study area and its rainfall stations.

### Material and Methods

#### Study Area

The study area is located in the Khazar watershed between 84°49'-54°41'E and 35°36'-37°19'N in northern Iran (Fig. 1). This area is bordered by the Caspian Sea to the north and has a mountain range in the southern region of the Khazar watershed. The mean annual precipitation varies from 1,400 mm in coastal areas to 300 mm in the Nemarestagh valley. The average elevation is 1,300 m above sea level. The climates of this area are subhumid and semiarid.

#### Data Sources

Data on rainfall amounts (daily, monthly, and annually) that had a minimal record length of 25 years were available at 86 stations. Rainfall data were collected from the Iran Meteorological Office. Of these 86 stations, only 20 stations recorded rainfall intensity. Rainfall intensity data for a 25-year period were obtained from the Water Resources Management Company.

Before using the collected data, they were controlled for homogeneity using Run's test.

#### Rainfall Erosivity Indexes

The  $EI_{30}$  index was computed for 20 synoptic stations of the study area. The kinetic energy ( $E$ ) was computed for these stations as follows:

$$E = \sum_{r=1}^k 0.29 [1 - 0.72 \exp(-0.05i_r)] \Delta V_r \quad (1)$$

...where  $i_r$  is rainfall intensity during the time interval ( $\text{mm}\cdot\text{min}^{-1}$ ) and  $\Delta V_r$  is the rainfall depth for  $r$  intervals [11]. The combination of  $E$  from Equation (1) and the maximum intensity for the 30-min intervals produces  $EI_{30}$ .

#### Parameters and Indexes Based on the Available Types of Precipitation Data

Combinations of the parameters based on rainfall amounts including annual rainfall, monthly rainfall, daily rainfall, or a combination as erosivity indexes were used for all 86 stations. The parameters used were as follows: mean annual rainfall ( $\bar{P}_{annual}$ ), mean monthly rainfall ( $\bar{P}_{month}$ ), maximum annual rainfall ( $P_{max.annual}$ ), maximum monthly rainfall ( $P_{max.monthly}$ ), maximum daily rainfall ( $P_{max.daily}$ ), standard deviation of annual rainfall ( $\delta_{annual}$ ), and standard deviation of monthly rainfall ( $\delta_{month}$ ).

Moreover, several indexes based on rainfall amount, such as the Fournier, Arnoldus, and Ciccacci indexes, were calculated for the 86 stations. The Fournier Index was calculated as follows:

$$FI = \frac{M_x^2}{P} \quad (2)$$

...where  $FI$  is the Fournier index,  $M_x$  is the mean monthly rainfall amount in mm, and  $P$  is the mean annual precipitation in mm [12]. The Arnoldus index (1980) or modified Fournier index was calculated as follows:

$$FI_{mod} = \sum \frac{P_i^2}{P} \quad (3)$$

...where  $FI_{mod}$  is the Arnoldus index,  $P_i$  is the mean monthly rainfall amount in mm, and  $P$  is the mean annual rainfall amount in mm [13]. The Ciccacci index was determined with the following equation:

$$C_i = \delta_{month} \cdot P \quad (4)$$

...where  $C_i$  is the Ciccacci index,  $\delta_{month}$  is the standard deviation of the monthly rainfall amount in mm, and  $P$  is the mean annual rainfall amount in mm [14].

#### Interpolation Methods

##### Kriging Method

It is necessary for the rainfall erosivity data to follow a normal distribution. The normality of the data was evaluated by the Kolmogorov-Smirnov test [7]. A semivariogram was used for the evaluation of the spatial correlation of the rainfall erosivity index by GS+ software. The semivariance that quantified spatial variations for all possible pairings of data was calculated by the following equation:

$$\gamma(h) = \frac{1}{2N(h)} \sum_{i=1}^{N(h)} \{Z(x_i) - Z(x_i + h)\}^2 \quad (5)$$

...where  $\gamma(h)$  is the semivariance at each lag (separating distance),  $N(h)$  is the number of point pairs separated by the given lag,  $z(x_i)$  is the measurement at location  $x_i$ , and  $z(x_i + h)$  is the measurement at  $x_i + h$ . The best model was fitted to semivariogram functions, and its range, sill, and nugget were optimized with the use of cross-validation [5].

##### Cokriging Method

Cokriging is an approach for incorporating secondary information, and cokriging is a multivariate extension of kriging. In this method, the correlations between the rainfall erosivity index and environmental variables that had an effect on the index are determined for selecting a covariable. Cokriging allows for the consideration of other environmental variables. Cokriging was determined as follows:

$$\gamma_{uv}h = \frac{1}{2} E[\{Z_u(x) - Z_u(x + h)\} \{Z_v(x) - Z_v(x + h)\}] \quad (6)$$

...where  $\gamma_{uv}$  is the cross-semivariance between  $u$  and  $v$ ,  $Z_u(x)$  is the primary variable, and  $Z_v(x)$  is the secondary variable [15].

Table 1. The correlation coefficient between  $EI_{30}$  and parameters/indexes based on rainfall amount in 20 synoptic stations.

	$\delta_{annual}$	$P_{max.annual}$	$\bar{P}_{annual}$	$\delta_{month}$	$P_{max.month}$	$P_{max.day}$	$FI$	$FI_{mod}$	$C_i$
$EI_{30}$	-0.33	-0.42	0.25	-0.29	-0.26	0.17	0.50	0.77**	0.34

\*\*means significant correlation at  $P < 0.01$ .

Table 2. The descriptive statistics of rainfall erosivity in the study area.

	Distribution type	min	max	mean	CV <sup>1</sup>	skewness	kurtosis
$EI_{30}$	lognormal	171	1446	870.65	46.20	-0.68	-0.46

<sup>1</sup>CV means coefficient of variations.

Unit of min, max and mean are  $MJ \cdot mm \cdot ha^{-1} \cdot h^{-1} \cdot y^{-1}$

The following three steps were used to implement the cokriging method:

- 1) semivariogram analysis of  $EI_{30}$
- 2) semivariogram analysis of covariable data
- 3) analysis of the cross-semivariogram

The semivariogram analysis for these three steps was carried out according to the kriging interpolation technique.

#### RBF Method

RBF methods are a series of exact interpolation methods in which the surface must go through each known value. There are five different functions in the Arc GIS software as follows: thin plate spline, spline with tension, completely regularized spline, multiquadratic function, and inverse multiquadratic function. Each basic function has a different shape and results in a slightly different interpolation surface. Each of the functions has a parameter that controls the smoothness of the surface. The appropriate function and number of parameters were selected with the use of the cross-validation technique.

#### IDW Method

IDW is the simplest interpolation method. A neighborhood around the interpolated point is identified, and a weighted average is taken of the observation values within the neighborhood. The weights are a decreasing function of distance. The property at each location without data is calculated by the following equation:

$$z = \frac{\sum_{j=1}^n z_j / d_{ij}^n}{\sum_{j=1}^n 1 / d_{ij}^n} \tag{7}$$

...where  $z_i$  is the property at location  $i$ ,  $z_j$  is the property at sampled location  $j$ ,  $d_{ij}$  is the distance from  $i$  to  $j$ ,  $n$  is the number of sampled locations, and  $n$  is the inverse distance weighting power [16].

### Comparative Performance of the Different Interpolation Methods

The validation of interpolation methods was evaluated by cross-validation and by a correlation of the map trend with actual trends. The cross-validation omitted a point and calculated the value of this location using the remaining points. The predicted and actual values at the location of the omitted point were compared. This procedure was repeated for a second point. Finally, the cross-validation was carried out by calculating the mean absolute error (MAE) and the root mean square error (RMSE) as follows:

$$MAE = \frac{1}{n} \sum |Z^* - Z| \tag{8}$$

$$RMSE = \frac{1}{n} \sqrt{\sum (Z^* - Z)^2} \tag{9}$$

...where  $Z^*$  is the estimated value,  $Z$  is the observed value, and  $n$  is the station number.

## Results and Discussion

### Rainfall Erosivity Index

It is necessary to generalize appropriate erosivity index ( $EI_{30}$ ) values for stations that lack rainfall intensity data. For this purpose, one may estimate  $EI_{30}$  from readily available rainfall parameters and erosivity indexes based on rainfall amount data. Thus, in 20 stations that had rainfall amount and intensity data, the following parameters and indices were calculated:  $\delta_{annual}$ ,  $P_{max.annual}$ ,  $\bar{P}_{annual}$ ,  $\delta_{month}$ ,  $P_{max.month}$ ,  $P_{max.day}$ , and several erosivity indexes based on rainfall amount, including  $FI$ ,  $FI_{mod}$ , and  $C_i$ . Moreover, the  $EI_{30}$  index was determined for these 20 stations. The correlation coefficients between  $EI_{30}$  and the parameters and indices based on a rainfall amount are presented in Table 1. Only  $EI_{30}$  was significantly correlated ( $r^2=0.75$  and  $P < 0.01$ ) with  $FI_{mod}$ . Therefore, a regional regression model was obtained for estimating  $EI_{30}$  as follows:

Table 3. Parameters of model fitted to semivariogram of  $EI_{30}$  and predicted error of kriging method.

Model	Range (km)		Angle (°)	$C_0+C$	$C_0$	$\frac{C_0}{C_0+C}$	Predicted error	
	major	minor		sill	nugget	nugget/sill	RMSE	MAE
Spherical	273.77	103.04	32	0.280	0.076	0.270	193.65	119.30

Unit of ( $C_0$ ) and ( $C_0+C$ ) is  $MJ \cdot mm \cdot ha^{-1} \cdot h^{-1} \cdot y^{-1}$

$$EI_{30} = -114.87 + 200.66 FI_{mod} \quad (10)$$

( $r = 0.72$  and  $P < 0.01$ )

As seen, this regression model showed that 72 percent of the variations  $EI_{30}$  are explained by  $FI_{mod}$ . Therefore, to generalize  $EI_{30}$  to all of the stations in the study area, the  $FI_{mod}$  index was computed from the other 66 stations without rainfall intensity data. The  $EI_{30}$  values were then calculated for the 66 stations using Equation 10.

### Interpolation Methods

The descriptive statistics of the rainfall erosivity index are shown in Table 2. The skewness (0.68) and coefficient of the Kolmogorov-Smirnov test ( $P < 0.05$ ) of rainfall erosivity revealed that these data did not have a normal distribution. A serious violation of data from the normal distribution may violate the variogram structure [17]. Therefore, the primary data of rainfall erosivity were transformed with a lognormal transformation. The Kolmogorov-Smirnov test ( $P > 0.05$ ) for the lognormal data verified a normal distribution.

An omnidirectional variogram of the  $EI_{30}$  data is shown in Fig. 2. A spherical model, which was the optimal model, was fitted to the semivariogram function by the minimal sum of the square of the residual ( $RSS = 0.007$ ). The properties of this model are shown in Table 3. The spherical model explained 87% of the variations of the semivariogram. Moreover, the nugget ( $C_0$ )-to-sill ( $C_0+C$ ) ratio of  $EI_{30}$  was 0.27. The ratio between 25 and 75 percentages represents the variable moderately spatial dependence [18].

Also, Baskan et al. [19] found this ratio is 0.32 for the soil erodibility factor semivariogram, which presents 32 percent of variability of soil erodibility factor that was unexplained [19].

There are different types of kriging methods. Ordinary kriging assumes that the constant average of statistical society is unknown, but the average is known in simple kriging. Also, universal kriging should only be used when there is a trend in the data. In this study, the semivariogram showed a constant sill and range, so there was no trend in the  $EI_{30}$  values. Moreover, the mean of the rainfall erosivity values was unknown. Therefore, the ordinary kriging method was suitable among the different types of kriging in this study.

A surface semivariogram in different directions is shown in Fig. 2. The elliptical contour lines present anisotropy and the concentric contour lines indicate isotropy [20]. The surface semivariogram in this study demonstrated that while the separation distance increases, the semivariance of  $EI_{30}$  has different trends at an azimuth of  $32^\circ$  when compared to the other directions. Therefore, rainfall erosivity showed anisotropy at  $32^\circ$ , which may be related to the heterogeneity of rainfall erosivity in this direction. Furthermore, the sill and nugget values of the  $EI_{30}$  semivariogram were 0.280 and 0.076, respectively, and were determined by the minimal RMSE (193.65) and MAE (119.30) (Table 3).

Another approach for incorporating secondary data is ordinary cokriging [5]. Different environmental factors such as elevation, latitude, and longitude may influence the rainfall erosivity index. The correlation coefficients for  $EI_{30}$  and the elevation, latitude, and longitude factors were 0.746, 0.126, and 0.178, respectively. Only elevation had a signifi-

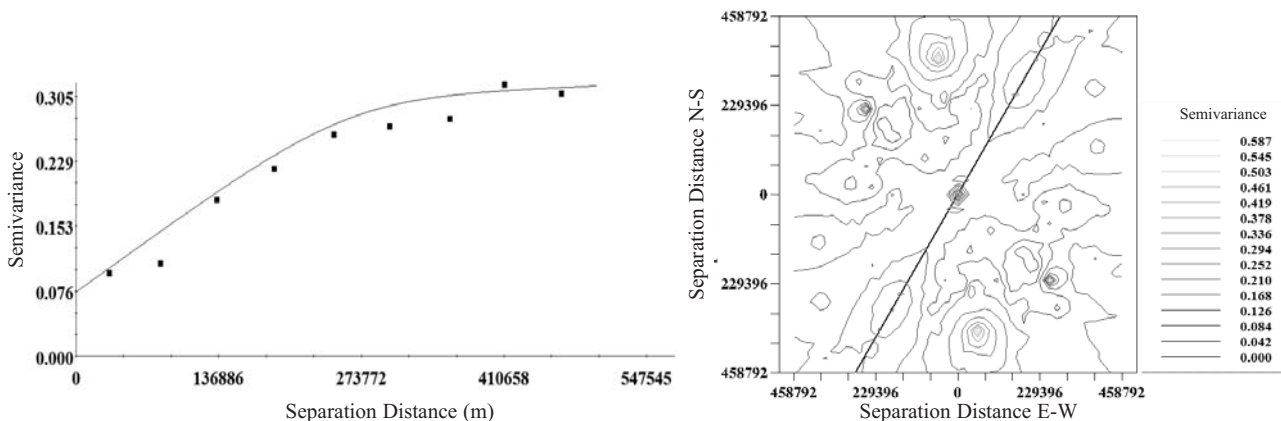


Fig. 2. Semivariogram (left) and surface semivariogram (right) of rainfall erosivity index.



Table 4. The parameters of semivariogram of elevation and cross semivariogram of  $EI_{30} \times Elevation$ .

	Model	Range (km)	Sill ( $C_0+C$ )	Nugget ( $C_0$ )	$\frac{C_0}{C_0+C}$	$r^2$
<i>Elevation</i>	Exponential	283	103,281	24,187	0.23	0.80
$EI_{30} \times Elevation$	Gaussian	293	25.5	5.0	0.19	0.71

Unit of sill and nugget is  $MJ \cdot mm \cdot ha^{-1} \cdot h^{-1} \cdot y^{-1}$

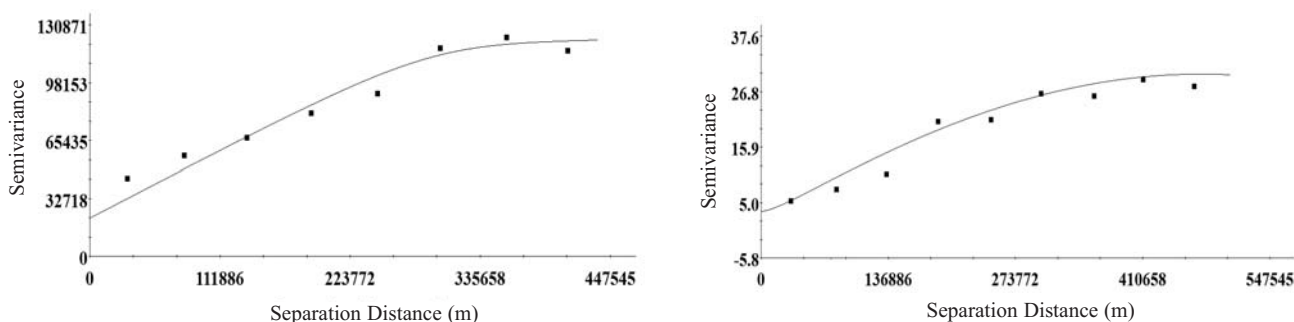


Fig. 3. Semivariogram of elevation as co-variable (left) and Cross semivariogram of  $EI_{30} \times Elevation$  (right).

cant correlation with  $EI_{30}$  at  $P < 0.001$ . Therefore, elevation was used as the covariable in the ordinary cokriging method.

A semivariogram of elevation and a cross-semivariogram of  $EI_{30} \times Elevation$  are shown in Fig. 3. The exponential model for elevation and the Gaussian model for  $EI_{30} \times Elevation$  were fitted by a Pearson correlation coefficient of 0.80 and 0.71, respectively. Moreover, the ratios of ( $C_0$ ) to ( $C_0+C$ ) of elevation and  $EI_{30} \times Elevation$  were 0.23 and 0.19, respectively, indicating strong spatial dependence (Table 4). These parameters were selected based on the minimal RMSE (187.57) and MAE (105.54).

In the RBF method, the minimal RMSE (195.77) and MAE (131.04) were obtained with the inverse multiquadratic equation and the optimized parameter number (1.35).

In the IDW method, the optimal power and number of neighborhood points were determined by means of the minimal estimating error. The results showed that the best power and numbers of neighborhood points for the  $EI_{30}$  index were 1 and 31, respectively, according to the minimal RMSE (210.07) and MAE (133.04).

### Comparative Performance of the Different Interpolation Methods

The cross-validation results of the different interpolation methods were compared (Fig. 4). The accuracy of the interpolation methods applied in this study was as follows: cokriging > kriging > spline > IDW. These results showed that the geostatistical methods (kriging and cokriging) were more accurate than the deterministic methods (IDW and spline). When compared to the cokriging method, the relative RMSE found for the kriging, spline and IDW methods was decreased by 3%, 4%, and 11%, respectively.

In all of the interpolation maps, the rainfall erosivity index had a decreasing trend from west to east that correlated with the climatic trend from subhumid to semiarid. The greatest surface area of watershed allocated to  $EI_{30}$  was in the range of 858-973  $MJ \cdot mm \cdot ha^{-1} \cdot h^{-1} \cdot y^{-1}$ , according to the map obtained by cokriging.

### Conclusions

$EI_{30}$ , a rainfall erosivity factor of the USLE equation, is important in erosion control and soil conservation. Computation of  $EI_{30}$  based on rainfall intensity requires intensity data at short intervals for a long period of time. However, access to short-term-interval rainfall intensity data in many parts of the world, especially in Iran, is limited [21]. In contrast, data based on rainfall amounts are usually available for longer periods. In this study,  $EI_{30}$  was estimated from the modified Fournier Index based on rainfall data.

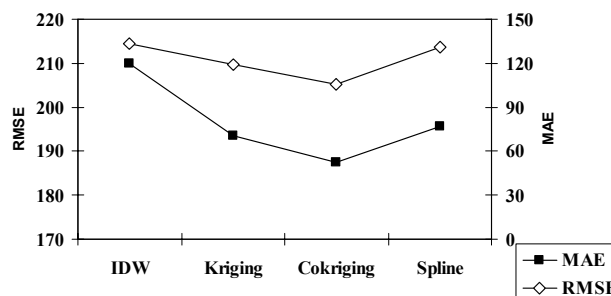


Fig. 4. Comparison of results of cross-validation for different interpolation methods.

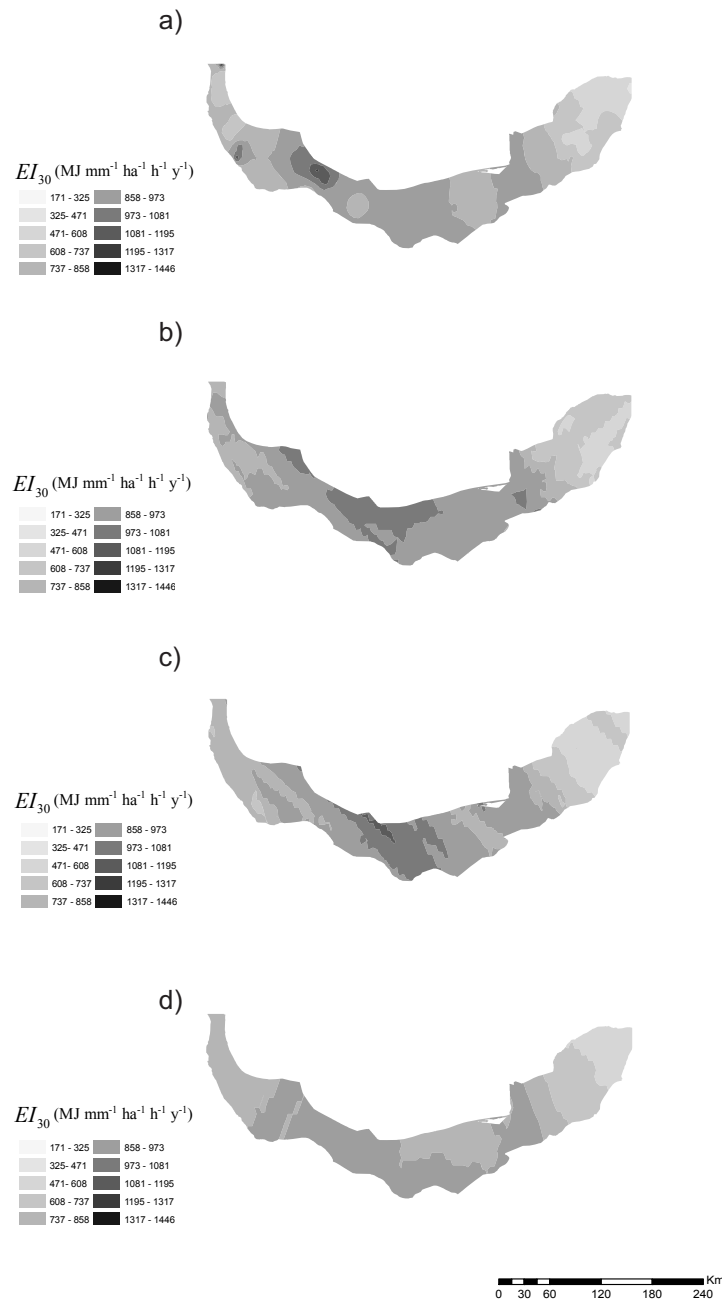


Fig. 5. Map of estimated rainfall erosivity by (a) IDW, (b) kriging, (c) cokriging, and (d) spline interpolation methods.

In the study area, the nugget-to-sill ratio of the  $EI_{30}$  values indicated a strong spatial correlation between the rainfall erosivity index values. Moreover, the cokriging method was the most precise interpolation method according to the minimal RMSE (187.57) and MAE (105.54).

The highest  $EI_{30}$  was observed in the western region, which has a humid climate. Rainfall erosivity had a decreasing trend from west (humid climate) to east (semi-arid climate), ranging from 171 to 1,450  $\text{MJ}\cdot\text{mm}\cdot\text{ha}^{-1}\cdot\text{h}^{-1}\cdot\text{y}^{-1}$ . Therefore, the spatial variations of rainfall erosivity are dependent on the spatial variability of the climate. The results from this study should be used in erosion models and conservation in this area with high rates of erosion.

### Acknowledgements

We are grateful to the Iran Meteorological Office and Water Resources Management Company for providing the necessary data sets.

### References

1. TOY T.J., FOSTER G.R., RENARD K.G. Soil Erosion: Processes, Prediction, Measurement, and Control. John Wiley & Sons, Inc., New York, **2002**.
2. HOYOS N., WAYLEN P.R., JARAMILLO A. Seasonal and spatial patterns of erosivity in a tropical watershed of the Colombian Andes. *J. Hydrol.* **314**, 177, **2005**.

3. SHAMSHAD A., AZHARI M.N., ISA M.H., WAN HUSSIN W.M.A., PARIDA B.P. Development of an appropriate procedure for estimation of RUSLE EI30 index and preparation of erosivity maps for Pulau Penang in Peninsular Malaysia. *Catena*. **72**, 423, **2008**.
4. BURROUGH P.A. GIS and geostatistics: Essential partners for spatial analysis. *Environ. Ecol. Stat.* **8**, (4), 361, **2001**.
5. GOOVAERTS P. *Geostatistics for natural resources evaluation*. New York, Oxford University Press, **1997**.
6. ZHANG K., HONG W., WU C-Z., DING X. Study on the Spatial Pattern of Rainfall Erosivity Based on Geostatistics and GIS of Fujian Province. *Journal of Mountain Science*. **27**, (5), 538, **2009**.
7. MEN M., YU Z., XU H. Study on the Spatial Pattern of Rainfall Erosivity Based on Geostatistics of Hebei Province, China. *Front Agric. China*. **2**, (3), 281, **2008**.
8. LLOYD C.D. Assessing the effect of integrating elevation data into the estimation of monthly precipitation in Great Britain. *J. Hydrol.* **308**, 128, **2005**.
9. VERWORN A., HABERLANDT U. Spatial interpolation of hourly rainfall effect of additional information, variogram inference and storm properties. *Hydrol. Earth Syst. Sci.* **15**, 569, **2011**.
10. DIODATO N., CECCARELLI M. Interpolation processes using multivariate geostatistics for mapping climatological precipitation mean in the Sannio Mountains (Southern Italy). *Earth Surface Processes and Landforms*. **30**, 259, **2005**.
11. BROWN L.C., FOSTER G.R. Storm erosivity using idealized intensity distributions. *Trans. A.S.A.E.* **30**, 379, **1987**.
12. COHEN M.J., SHEPHERD K.D., WALSH M.G. Empirical formulation of the universal soil loss equation for erosion risk assessment in a tropical watershed. *Geoderma*. **124**, 235, **2005**.
13. ARNOLDUS H.M.J. An Approximation to the Rainfall Factor in the Universal Soil Loss Equation. In: De Boodt M, Gabriels M (Eds) *Assessment of Erosion*, Wiley, Chechester: UK, pp. 127-132, **1980**.
14. CICCACCI S., FREDI P., LUPIA PALMIERI E., PUGLIESE F. Indirect evaluation of erosion entity in drainage basins through geomorphic, climatic and hydrological parameters. *International Geomorphology*. **2**, 33, **1986**.
15. TAGHIZADEH MEHRJARDI R., ZAREIAN JAHROMI M., MAHMODI S.H., HEIDARI A. Spatial distribution of groundwater quality with geostatistics (case study: Yazd-Adrakan Plain). *World Appl. Sci. J.* **4**, (1), 9, **2008**.
16. LU G.Y., WONG D.W. An adaptive inverse-distance weighting spatial interpolation technique. *Comput. Geosci-Uk*. **34**, 1044, **2008**.
17. OUYANG Y., ZHANG J.E., OU L.T. Temporal and spatial distributions of sediment total organic carbon in an estuary river. *J. Environ. Qual.* **35**, (1), 93, **2006**.
18. CAMBARDELLA C. A., MOORMAN T. B., NOVAK J. M., PARKIN T. B., KARLEN D. L., TURCO R. F., KONOPKAA. E. Field-scale variability of soil properties in Central Iowa soils. *Soil Science Society of America Journal*. **58**, 1501, **1994**.
19. BASKAN O., CEBEL H., AKGUL S., ERPUL G. Conditional simulation of USLE/RUSLE soil erodibility factor by geostatistics in a Mediterranean catchment, Turkey. *Environ. Earth. Sci.* **60**, (6), 1179, **2010**.
20. WANG G., GERTNER G., SINGH V., SHINKAREVA S., PARYSOW P., ANDERSON A. Spatial and temporal prediction and uncertainty of soil loss using the revised universal soil loss equation: a case study of the rainfall-runoff erosivity R factor. *Ecol. Model.* **153**, 143, **2002**.
21. YU B., HASHIM G.M., EUSOF Z. Estimating the r-factor with limited rainfall data: a case study from peninsular Malaysia. *J. Soil. Water. Conserv.* **56**, 101, **2001**.